Wet Antecedent Conditions and High Baseflow Trigger Widespread Floods in Indian Sub-continental River Basins

Nanditha J. S.[1] and Vimal Mishra[1,2]

[1]Civil Engineering, Indian Institute of Technology Gandhinagar, Gandhinagar, 382355, India

[2]Earth Science, Indian Institute of Technology Gandhinagar, Gandhinagar, 382355, India

Corresponding author: Vimal Mishra, vmishra@iitgn.ac.in

Key points

- There is a high probability of widespread flooding (>15%) in the peninsular river basins in India.
- Moist antecedent conditions and streamflow seasonality determine the timing and probability of widespread floods.
- The variability in the probability of widespread flooding across different river basins depends on the extremeness of flood peaks

Abstract

Widespread floods affecting multiple subbasins in a river basin are more disastrous than localized flooding. Understanding the mechanisms, drivers and probability of widespread flooding is pertinent for devising suitable policy measures. Here, we investigate the occurrence and drivers of widespread flooding in seven Indian sub-continental river basins during the observed climate (1959-2020). We use a novel methodology for determining widespread floods and a non-stationary extreme value distribution to identify the mechanisms of widespread flooding. We find that the peninsular river basins have a high probability of widespread flooding, while the transboundary basins of Ganga and Brahmaputra have a low probability. In addition to wet antecedent conditions, the relative rareness of high flows across different subbasins is crucial in explaining the variability of widespread flood probability across different river basins. Our results show that favourable antecedent baseflow and soil moisture conditions, uniform precipitation distribution, and streamflow seasonality determine the seasonality and probability of widespread floods. Further, widespread floods are associated with large atmospheric circulations, resulting in near-uniform precipitation within a river basin. Moreover, we found no significant relation

between widespread floods and oceanic circulations. Our findings highlight the prominent drivers and mechanisms of widespread floods with implications for flood mitigation in India.

Keywords: widespread floods, antecedent soil moisture, baseflow, non-stationary flood modelling, flood drivers, flood mechanisms

1. Introduction

Flood is a predominant natural disaster in India, with more than 390 million people exposed to a high risk of flooding (Rentschler et al., 2022). India receives 80% of the total annual rainfall in four months during the southwest monsoon season from June to September. Consequently, the country faces the most devastating floods during the same period (Nanditha & Mishra, 2022). The high seasonality of the precipitation increases the risk of spatially and temporally coherent flood events. Widespread flooding that simultaneously covers a large part of a river basin can have a higher socio-economic risk than localized flooding. The more disastrous widespread floods reportedly have an entirely different causative mechanism (Bertola et al., 2020; Merz et al., 2021). However, understanding the occurrence and drivers of widespread floods in the Indian sub-continental river basins is limited as the focus has primarily been on localized flooding (Lamb et al., 2010).

Riverine floods are driven by multiple factors, including spatial and temporal distribution of precipitation, antecedent soil moisture conditions, catchment characteristics, and river system infrastructures like reservoirs and levees (Berghuijs et al., 2016, 2019; Günter Blöschl et al., 2015; Merz et al., 2021; Sharma et al., 2018; Tarasova et al., 2019). The complex interaction of land and atmospheric factors in the generation of floods is often cited as a reason for precipitation trends not translating to floods in most global river basins (Alfieri et al., 2017; Bloschl, 2022; Sharma et al., 2018; van der Wiel et al., 2018). Wet antecedent conditions due to prolonged precipitation, rain on snow events that effectively increase infiltration excess flows, and snow melts are directly associated with high flows compared to extreme precipitation (Berghuijs et al., 2016; Günter Blöschl et al., 2019; Ivancic & Shaw, 2015; Tramblay et al., 2021; Wasko & Nathan, 2019). Therefore, extreme precipitation and land surface conditions play a significant role in determining the occurrence of localized flooding. However, widespread flood events could be driven by an entirely different causative mechanism.

The occurrence and drivers of widespread flooding have recently received considerable attention due to loss and damages caused by them (Di Capua et al., 2021, Fazel-Rastgar, 2020, Merz et al., 2021; Nanditha et al., 2023, Vijaykumar et al., 2021). The causative hydrometeorological factors of devastating floods have been recognized (Hong et al., 2011; Lyngwa & Nayak, 2021; Martius et al., 2013; Vijaykumar et al., 2021). For instance, the 2010 Pakistan flood and its teleconnection with the 2010 European heatwave and atmospheric blocking has been established (Hong et al., 2011; Martius et al., 2013). The 2018 Kerala floods, 2022 Pakistan floods, and lower Mississippi river floods are reportedly associated with atmospheric rivers that usually carry moisture from the tropics and debouch it to the extratropics (Lyngwa & Nayak, 2021; Nanditha et al., 2023; Su et al., 2023). We hypothesize that widespread flooding is associated with widespread extreme precipitation, concomitantly to large-scale atmospheric circulations apart from the favorable land surface and catchment characteristics.

In Indian river basins, where rainfall is the dominant precipitation mechanism, wet antecedent soil moisture is vital in driving high flows (Garg & Mishra, 2019; Nanditha et al., 2022). Therefore, multiple-day precipitation is a prominent flood driver than short-duration extreme precipitation (Nanditha & Mishra, 2022). However, the relative role of different drivers can vary for widespread floods as they are spatially and temporally coherent across a large river basin area. For instance, Brunner et al. (2020) reported a high susceptibility to widespread flooding in basins with a highly seasonal flow regime and uniform climatic conditions in the United States (US). Most Indian sub-continental river basins exhibit a seasonal flow regime; therefore, there could be a considerable risk of widespread flooding, which has not yet been examined. Further, there are substantial differences in the climatic and catchment characteristics across the Indian subcontinental river basins, making it pertinent to understand the mechanisms that would cause widespread floods. Moreover, considerable variability in the spatial and temporal precipitation pattern is observed over the Indian subcontinent related to climate change and direct human interventions (Goswami et al., 2006; Vinnarasi & Dhanya, 2016a). Since climate change is projected to alter the intensity and frequency of extreme precipitation, evaluating the drivers of widespread flooding in the observed climate is imperative (Ali & Mishra, 2018; Krishnamurthy et al., 2009). Here, we aim to address the crucial research gaps associated with the occurrence, drivers, and mechanisms of widespread floods in the Indian river basins. We specifically address the following research questions: (1) What is the probability of widespread flooding in Indian river basins? (2) Is there any

variability in the seasonal distribution of widespread floods? and (3) what are the prominent drivers of the widespread floods in Indian river basins?

2. Data and methods

The Variable Infiltration Capacity (VIC) model

Indian sub-continental river basins are considerably influenced by human interventions (e.g., reservoirs and irrigation). Hence, there needs to be more consistent records of long-term observed daily flow that is crucial to examine the occurrence of widespread floods. Therefore, we conducted simulations of hydrological variables. We used the calibrated Variable Infiltration Capacity (VIC) hydrological model at 0.25° to simulate daily streamflow and soil moisture (Liang et al., 1994; 1996). The VIC model is a semi-distributed land surface model that solves the energy and water budget at each grid cell. Further, the gridded output from the VIC model is routed using a routing model that uses 1-D St Venant equations to obtain simulated streamflow at specific locations (Lohmann et al., 1996). We obtained the daily meteorological forcing (precipitation, maximum and minimum temperatures) required for the VIC model from the India Meteorological Department (IMD). We used daily gridded precipitation (Pai et al., 2014) at 0.25° and maximum and minimum temperatures (Srivastava et al., 2009) from IMD for the 1951-2020 period. The gridded precipitation and temperature products are developed by interpolating station observations, which include 6995 rain gauges and 395 temperature stations. We used streamflow observations from India Water Resources Information System (IWRIS) to evaluate the performance of the VIC model. The model is calibrated at 23 sub-basins across the seven major river basins in India, where consistent and long-term records of streamflow observations are available (Nanditha & Mishra, 2022). The model performance is evaluated using Nash-Sutcliffe efficiency (NSE) [Nash & Sutcliffe, 1970] and coefficient of correlation (r). We obtained NSE above 0.6, and r above 0.75 for most locations (Table S1), which signifies the satisfactory performance of the VIC model to simulate daily streamflow. Moreover, the VIC simulated annual maximum flow is also well correlated with the observations (Figure S1).

Identification of widespread flooding

We considered seven major river basins in the Indian subcontinent, including Ganga, Brahmaputra, Godavari, Krishna, Mahanadi, Narmada, and Cauvery (Figure 1). As we aim to examine the occurrence and drivers of the widespread floods, smaller (coastal) river basins are not considered for the analysis. In the selected seven river basins, we identified 73

129 subbasins so that the contributing area is as distinct as possible using the Hydroshed subbasin
130 and stream network dataset (Lehner, B., 2013). The subbasins closer to the outlet have a
131 considerable overlapping area with the subbasins upstream in the river basins. Therefore, we
132 estimated the unique contributing area to each subbasin within a river basin. We used a peak
133 over a threshold (POT) methodology and estimated the top one percentile flow events (high
134 flows that exceed the 99th percentile) in each of these 73 sub-basins. Events separated by 15
135 days were considered to ensure independence between selected events. For each event, we
136 estimated the unique area weighted fraction, *f,* of a basin that experiences high flow during
137 that particular event (equation 1).

138 $$f = \frac{\sum A_i I_i}{\sum A_i} \qquad \ldots\ldots\ldots\ldots\ldots\ldots (1)$$

A_i = unique contributing area to each subbasin

I_i = binary indicator; 1 if the subbasin, i register high flow (top 1 percentile) during the particular event and 0 otherwise.

139 We consider a lag period of ±3 days to account for the lag time for the peak flow to reach
140 different outlet points (Nanditha & Mishra, 2022). If *f* is greater than or equal to 0.5, the
141 particular event was identified as a widespread flood event. Brunner et al. (2020) used a
142 simple fraction to determine widespread floods within a river basin. We modified the method
143 and used an area-weighted fraction that accounts for the difference in the area of different
144 subbasins. Further, the probability of widespread flooding was estimated as the ratio of
145 widespread floods to the total high-flow events within a river basin.

146 **Flood frequency analysis**

147 The widespread flood in a river basin can occur as: (1) rare events at a few subbasins drive
148 high flow across the different downstream subbasins, and (2) simultaneous occurrence of
149 high flow events with lower return periods in multiple subbasins. We fit an extreme value
150 distribution to each subbasin's annual maximum flow time series. We use Generalized
151 Extreme Value (GEV) distribution as it is suitable for block maxima-based extreme value
152 time series (Coles, 2001; Katz et al., 2002). We considered stationary and a couple of non-
153 stationary models with time [Non-Stationary Type I to III] and standardized departure of
154 annual maximum precipitation [Non-Stationary Type IV to VI] as covariates [c(t)]. We used

155 the extRemes package in R (Gilleland & Katz, 2016) and the maximum likelihood estimation
156 method to fit the distribution (Table S2).

157 Stationary model:

158 $$GEV = f(\mu, \sigma, \varepsilon) \quad \ldots\ldots\ldots\ldots\ldots\ldots (2)$$

159 where μ is the location, σ is the scale, and ε is the shape parameter of the model.

160 Time [*t*] and standardized departure of annual maximum precipitation [*p(t)*] for each sub-
161 basin were used as covariates [*c(t)*] for the non-stationary models. We consider linear
162 variation in the location, scale, and shape parameters. In Non-stationary type I and IV
163 models, we used a time-varying location parameter with time and precipitation as covariates
164 and constant scale and shape parameters (equations 3-4). In type II and V models, we used
165 time-varying location and scale parameters with a constant shape parameter (equations 4-6);
166 in type III and VI models, we used time-varying location, scale, and shape parameters
167 (equations 4,6-8). We find that 19 subbasins exhibited non-stationarity in the annual
168 maximum flow based on the likelihood-ratio test (at 95% significance level) and Akaike and
169 Bayesian Information Criterion (AIC, BIC) [Table S2, Coles, 2001; Ouarda & Charron,
170 2019].

171 Non-stationary Type I and IV:

172 $$GEV = f(\mu(t), \sigma, \varepsilon) \quad \ldots\ldots\ldots\ldots\ldots\ldots (3)$$

173 $$\mu(t) = \mu_0 + \mu_1 c(t) \quad \ldots\ldots\ldots\ldots\ldots\ldots (4)$$

174 Non-stationary Type II and V:

175 $$GEV = f(\mu(t), \sigma(t), \varepsilon) \quad \ldots\ldots\ldots\ldots\ldots\ldots (5)$$

176 $$\sigma(t) = |\sigma_0 + \sigma_1 c(t)| \quad \ldots\ldots\ldots\ldots\ldots\ldots . (6)$$

177 Non-stationary Type III and VI:

178 $$GEV = f(\mu(t), \sigma(t), \varepsilon(t)) \quad \ldots\ldots\ldots\ldots\ldots (7)$$

179 $$\varepsilon(t) = \varepsilon_0 + \varepsilon_1 c(t) \quad \ldots\ldots\ldots\ldots\ldots\ldots (8)$$

180 **Soil moisture, baseflow, and atmospheric variables**

181 Next, we examined the soil moisture, baseflow, and atmospheric conditions before the
182 widespread floods to understand the atmospheric and catchment characteristics associated

with the events. Basin averaged seven-day mean soil moisture (~30 cm soil layer) simulations from the VIC model were used to assess the antecedent soil moisture conditions. We used Eckhardt digital filter to determine the baseflow component (Eckhardt, 2005, equation 9), which classifies high frequency fluctuations in streamflow to quick flow and the slow frequencies to baseflow (Eckhardt, 2008). Baseflow measurements are difficult to obtain, therefore, it is challenging to assess the accuracy of any baseflow identification methods. Xie et al. (2020) evaluated different baseflow separation methods based on the strict baseflow points (the points where the quick flow and interflow cease to exist) constructed using streamflow observations in catchments across the contiguous USA. They found the two-parameter-based Eckhardt digital filter performs well without using hydrogeological parameters of a catchment in the equation. The filter requires the recession constant, α, and maximum baseflow index (BFI_{max}) for estimating baseflow from total runoff. BFI_{max} depends on the hydrological and geological characteristics of the basin. However, without these datasets, BFI_{max} can be estimated using the recession constant by applying a backward pass (Collischonn & Fan, 2012)[equations 10 and 11].

$$b_i = \frac{\alpha b_{i-1}(1-BFI_{max})+(1-\alpha)Q_i BFI_{max}}{1-\alpha BFI_{max}} \quad \text{.....(9)}$$

subject to $b_i \leq Q_i$

$$b_{i-1} = \frac{b_i}{\alpha} \quad \text{.....(10)}$$

$$BFI_{max} = \frac{\sum Q_i}{\sum b_i} \quad \text{.....(11)}$$

subject to a maximum of 0.8 suggested by Eckhardt (2008) for perennial and porous aquifers.

Where Q_i is the total runoff or streamflow, and b_i is the baseflow at the i^{th} instant.

BFI_{max} estimated for each subbasin is listed in the supplementary Table S3. We used a recession constant, α=0.95, uniformly for all the subbasins. A lower α and BFI_{max} are reported to improve the baseflow comparison with strict baseflow points; therefore, we used a uniform α = 0.95 (Xie et al., 2020). However, optimizing the values of α and BFI_{max} based on the hydroclimatological characteristics of a basin can further provide robust estimates.

Atmospheric variables from the European Reanalysis (ERA 5) [Hersbach & Dee, 2016] is used to evaluate the atmospheric conditions before widespread flood events. We estimated the vertically integrated moisture transport using the eastward and northward components of

moisture flux variables (q_u and q_v) [$Equation$ 12]. We also estimated the mean seal level pressure anomalies considering 1991-2020 as the reference period.

$$IVT = \sqrt{q_u^2 + q_v^2} \quad \ldots\ldots\ldots\ldots\ldots\ldots (12)$$

Sea surface temperature (SST) anomalies in the eastern Pacific and the Indian Ocean regions are associated with the annual variability in the summer monsoon (JJAS) season precipitation over India (B. Goswami, 1998; Saji et al., 1999; Walker, 1925). We obtained Nino 3.4 index and Indian Ocean Dipole (IOD) Mode Index from the NOAA National Weather Service (NWS) Climate Prediction Centre (CPC) and Australian Bureau of Meteorology, respectively to evaluate the association of SST anomalies with the occurrence of WF events (Nanditha et al., 2022).

3. Results

3.1. The probability of widespread flooding

First, we examined the probability of widespread flooding in the Indian subcontinental river basins from 1959-2020. Peninsular river basins have a high likelihood of widespread flooding, with the Narmada basin (35%) topping the list, followed by Mahanadi (31% each), Godavari (22%), Cauvery (18%) and Krishna (16%) [Figure 1]. In contrast, the Ganga basin has the least probability (3%), while the Brahmaputra has a slightly higher probability (8%) [Table S5]. We estimated widespread flood probability in each decade from 1961-2020 to further understand interdecadal changes in the probability. We did not find any significant trend in decadal probability across the seven river basins from 1961 to 2020 (Figure 1). While the Narmada and Mahanadi basins show a slight increase in the probability towards the end of the observational period, the Brahmaputra River basin has experienced a decline in the last three decades (1991-2020). Overall, there was no significant trend in widespread flooding in the Indian sub-continental river basins during 1959-2020.

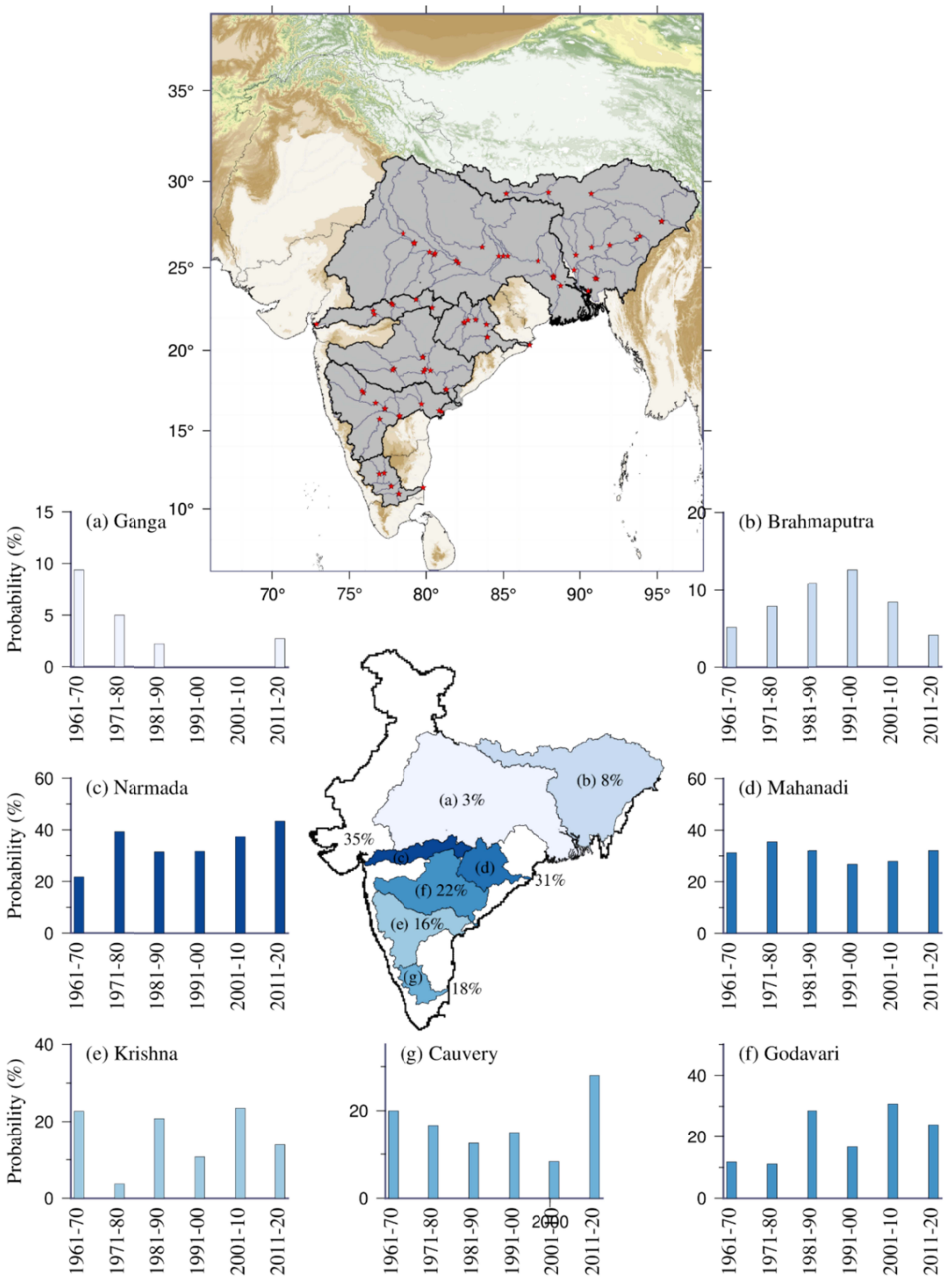

Figure 1. **Study area and WF probability.** We used 73 subbasins in the seven major river basins. The black line and thin grey lines indicate the boundary of major basins and sub-basins, respectively. The red asterisk indicates the sub-basin outlets. (a-g) show the change in WF probability per decade from 1961-2020 in seven major basins.

The high variability in the probability of widespread flooding among the Indian sub-continental river basins indicates the role of various catchment and atmospheric characteristics of a river basin. The catchment characteristics such as slope, area, stream

density, river network, and soil types determine the connectivity within different subbasins and the time required for the peak flows in upstream basins to reach the downstream basins (Brunner et al., 2020; Sharma et al., 2018; Sofia & Nikolopoulos, 2020; Wang et al., 2021). The hydrological characteristics like the flow regime of a basin and the antecedent moisture conditions of the catchment in terms of soil moisture, baseflow, and rainfall, have a significant influence on flood peaks (Berthet et al., 2009; Bloschl, 2022; Pathiraja et al., 2012; Wasko et al., 2020; Wasko & Nathan, 2019). Similarly, the atmospheric and climatic characteristics also influence the timing and magnitude of flood peaks and hence would influence widespread flooding (Brunner et al., 2020; Su et al., 2023). Here, we focus on the atmospheric and land surface processes that drive the widespread flooding pattern across the river basins. We specifically consider the role of streamflow seasonality, spatial and temporal precipitation patterns, and antecedent soil moisture and baseflow conditions before the flood-driving storms.

3.2 Role of rainfall and streamflow seasonality

Next, we evaluate the seasonal pattern of widespread flood probability in the Indian sub-continental river basins to unravel the role of streamflow seasonality. August is the only month in which widespread floods occur in all seven river basins. August has the highest widespread flood probability in the Indian sub-continental river basin except in the Krishna River basin (Figure 2). Godavari, Mahanadi, and Narmada basins experience widespread flooding in the summer monsoon months of July, August, and September (Figure 2j, l, m). Most subbasins in Cauvery receive rainfall during the northeast monsoon season (October-December); hence, widespread flooding in the basin occurs from June to December (Figure 2g, n). Notwithstanding high flows occurring in the non-monsoon season, widespread floods occur only in the summer monsoon months in the Brahmaputra basin. Therefore, the widespread flood probability during the summer monsoon (JJAS) is around 9% in the Brahmaputra basin. The highest frequency of widespread floods in the basin occurs in August, with a probability of 15% (Figure 2b, I, Table S5). Our results show a strong seasonality in the WF probability in the subcontinental river basins.

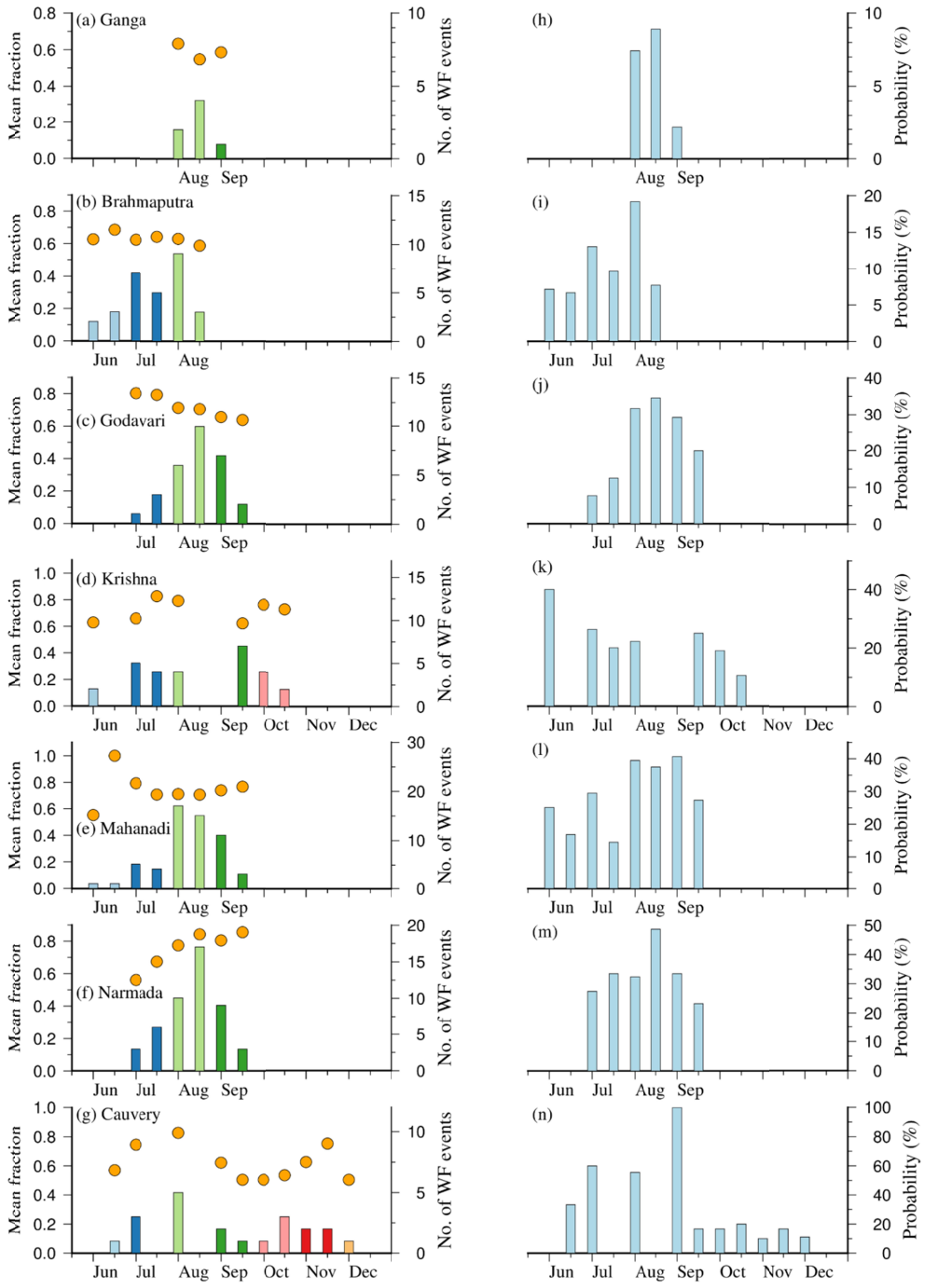

Figure 2. Seasonality of WF flooding. Figures a-g show the seasonal distribution of widespread floods (colored bars) in each basin from 1959-2020. Every month is sliced into two halves for analysis. The orange circles show the mean fraction of the basin area that experiences widespread flooding in each biweekly period. Figures (h-n) show the corresponding WF probability in each biweekly period.

279 The seasonality in the widespread flood probability is related to the temporal rainfall
280 distribution pattern over India. India receives around 80% of the total annual precipitation
281 during the monsoon season from June-September (Shukla & Huang (2016), Figure 3). While
282 the Brahmaputra basin receives precipitation much early during the season, the Cauvery basin
283 receives most precipitation from October to December in the northeast monsoon season
284 (Fukushima et al., 2019). The rest of the basins receive precipitation mainly during the
285 summer monsoon season (June-September). Therefore, the widespread flood probability
286 during the monsoon season differs greatly from the annual probability except in the Cauvery
287 basin. In the Cauvery basin, the widespread probability increases by more than 50% during
288 the summer monsoon season (Table S5). Relatively few high-flow events occur during the
289 summer monsoon season in the basin, but most of those events cause widespread flooding,
290 thereby increasing the WF probability during the monsoon season. In general, all basins
291 ubiquitously exhibit high widespread flood probability in the summer monsoon months from
292 June to September. Therefore, it becomes imperative to understand the reason for the high
293 WF probability in the peak monsoon months in most river basins. Henceforth, we examine
294 the role of rainfall distribution and antecedent moisture conditions.

295 Next, we evaluate the role of rainfall patterns that could explain the seasonality and
296 variability in widespread flooding across the river basins. The peninsular rivers of Narmada,
297 Mahanadi and Godavari lie in the core monsoon region and receive more rainy days during
298 the summer monsoon season with the least spatial variability (coefficient of variation less
299 than 14%) [Figure 3]. Further, the median inter-storm duration between rainy days (>5mm)
300 ranges from 3-4 days in these basins (Table S6). Therefore, continuous dry days are relatively
301 lower in these three central Indian basins. Even though the Brahmaputra basin receives the
302 highest number of rainy days, the spatial variability is relatively higher (Figure 3a-b). The
303 upper parts of the basin receive relatively low total precipitation implying that these regions
304 receive temporally distributed low-intensity precipitation (< 35 mm) [Figure 3a-b, S2b].
305 Similarly, the upper subbasins in the eastern part of the Ganga basin have lower rainy days
306 resulting in a high coefficient of variability. But the spatial pattern of rainy days in the
307 summer monsoon season over the Gangetic basin is similar to the total rainfall distribution in
308 the same season, unlike the Brahmaputra basin. Thus, the Ganga River basin experiences
309 high spatial variability in rainy days as well as in total rainfall. Therefore, the uniform
310 distribution of precipitation across the river basins of Narmada, Mahanadi, and Godavari
311 plays a predominant role in translating the high flows in these basins to widespread flooding.

Hence, the location of these catchments in central India, a core monsoon region, increases the probability of widespread floods in these basins.

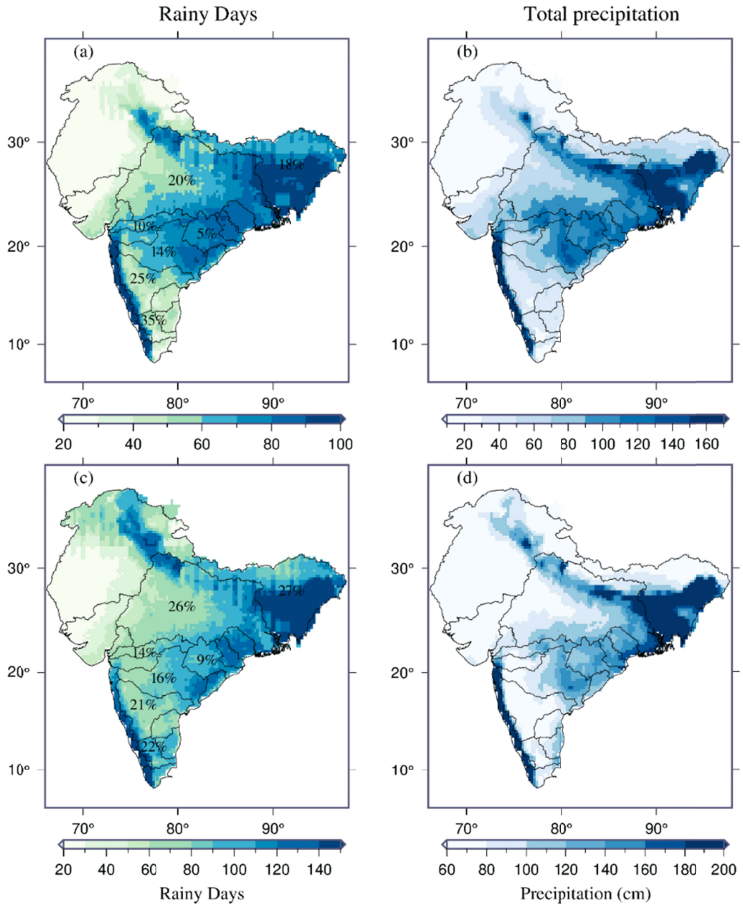

Figure 3. Climatology of rainy days and total precipitation. Figure (a) shows the climatology of rainy days during the summer monsoon season (June-September) across the Indian subcontinental river basins. The numbers indicate the spatial coefficient of variation, CV of rainy days within each basin. CV is estimated as the ratio of the standard deviation of rainy days within each basin to the average rainy days in each basin. $[CV = 100 * std(rainy\ days)/mean(rainy\ days]$. Figure b shows the climatology of total monsoon season precipitation. Figures (c-d) is same as (a-b), but for the calendar year (January-December).

The Cauvery and Krishna River basins have a relatively high coefficient of variation (CV) during the summer monsoon season compared to the other peninsular rivers. Therefore, the widespread flood probability in Krishna is lower than in other peninsular rivers. Considering the total annual precipitation, there is less variability on rainy days in Cauvery and Krishna than Ganga and Brahmaputra basins (Figure 3). Thus, Krishna and Cauvery show higher WF

probability than Ganga and Brahmaputra basins. However, Cauvery has a higher WF probability during the monsoon season (~31%) [Table S5]. The high WF probability of Cauvery during the monsoon season could be more related to catchment size than spatial distribution of precipitation. Cauvery is the smallest basin considered in the study, with a catchment area of 81,155 km^2. Consequently, the chance for simultaneous occurrence of high flows increases across the subbasins due to the relatively uniform distribution of flood-driving storms (G Blöschl et al., 2007; Sharma et al., 2018). We find that the spatial distribution of rainfall can explain the variability of WF probability across different river basins. However, to understand the reason for the high WF probability during the monsoon season, we investigate the catchment moisture conditions prior to widespread flooding.

3.3.Role of antecedent soil moisture and baseflow

We examine the antecedent soil moisture and baseflow conditions prior to the major precipitation event associated with all high-flow events in the river basins to understand the linkage between catchment processes and widespread floods. We find that a relatively high soil moisture percentile prevailed in all the subbasins before the storms that caused widespread flooding compared to those that did not result in widespread floods (Figure 4 a-g). The seven-day mean soil moisture above the 95^{th} percentile persisted before widespread floods in all the river basins except for Cauvery. Further, we observe low variability in soil moisture percentiles across the subbasins among the peninsular rivers excluding Cauvery. We find that the probability of widespread flooding increases when the catchment averaged soil moisture percentiles are higher. A higher antecedent soil moisture condition prevails due to storms occurring before the specific event or higher humidity during the monsoon season that reduces the bare soil evaporation (Pathiraja et al., 2012; Tramblay et al., 2021).

Similar to soil moisture, the persistence of higher antecedent baseflow conditions is observed to increase the probability of widespread flooding in a river basin (Figure 4 h-n). The baseflow component in the river basins peaks in the middle of the summer monsoon season in most basins because of sustained precipitation. The antecedent baseflow significantly influences flood peaks (Ettrick et al., 1987; Merz et al., 2021). Similarly, wet antecedent soil moisture conditions play a crucial role in driving high flows (Berghuijs et al., 2016; Hettiarachchi et al., 2019; Kim et al., 2019; Nanditha & Mishra, 2022; Wasko & Nathan, 2019). The summer monsoon season precipitation begins towards the end of May in the Brahmaputra basin to early July in the Narmada basin (IMD). Therefore, the wet antecedent

conditions occur by the end of July and early August due to continuous precipitation. Similarly, the baseflow fraction of the total runoff also increases, providing favorable conditions for widespread floods across the basins. Further, an increase in rainy days could sustain favorable conditions, whereas long break spells may cause soil drying and a dip in the baseflow components (Ettrick et al., 1987; Sharma et al., 2018). Overall, the antecedent soil moisture and baseflow conditions explain the seasonality of widespread floods in all the river basins.

The widespread flood probability depends on the area fraction and POT thresholds used to identify the events. We assessed the sensitivity of widespread flood probability to POT thresholds (98,99, 99.5, 99.8 and 99.9) and area fraction (0.5, 0.6, 0.7,0.8,0.9 and 1) [Figure S3]. As expected, the WF probability reduces with an increase in area fraction and the POT thresholds in most basins. The peninsular river basins of Godavari, Cauvery, and Narmada exhibit a high probability (>10%) of more severe (>99.9 percentile) widespread flooding. We observe non-occurrence of severe widespread flooding and widespread flooding that cover a large basin fraction (>0.7) in the Ganga basin. The Cauvery river basin shows a low sensitivity of widespread probability to flood severity (~18% widespread flood probability for 99.9 POT thresholds) [Figure S3]. We analyzed the seasonal pattern of WF probability and studied the possible drivers, including streamflow seasonality, the spatial distribution of rainy days, and antecedent moisture conditions. We found the streamflow seasonality and antecedent moisture conditions explain the observed seasonality of widespread flooding. The spatial distribution of rainfall and rainy days could explain the variability of widespread flood probability across the major river basins. However, constant catchment characteristics like the stream network pattern, stream density, and slope can further explain the variability observed in the flooding pattern (Brunner et al., 2020).

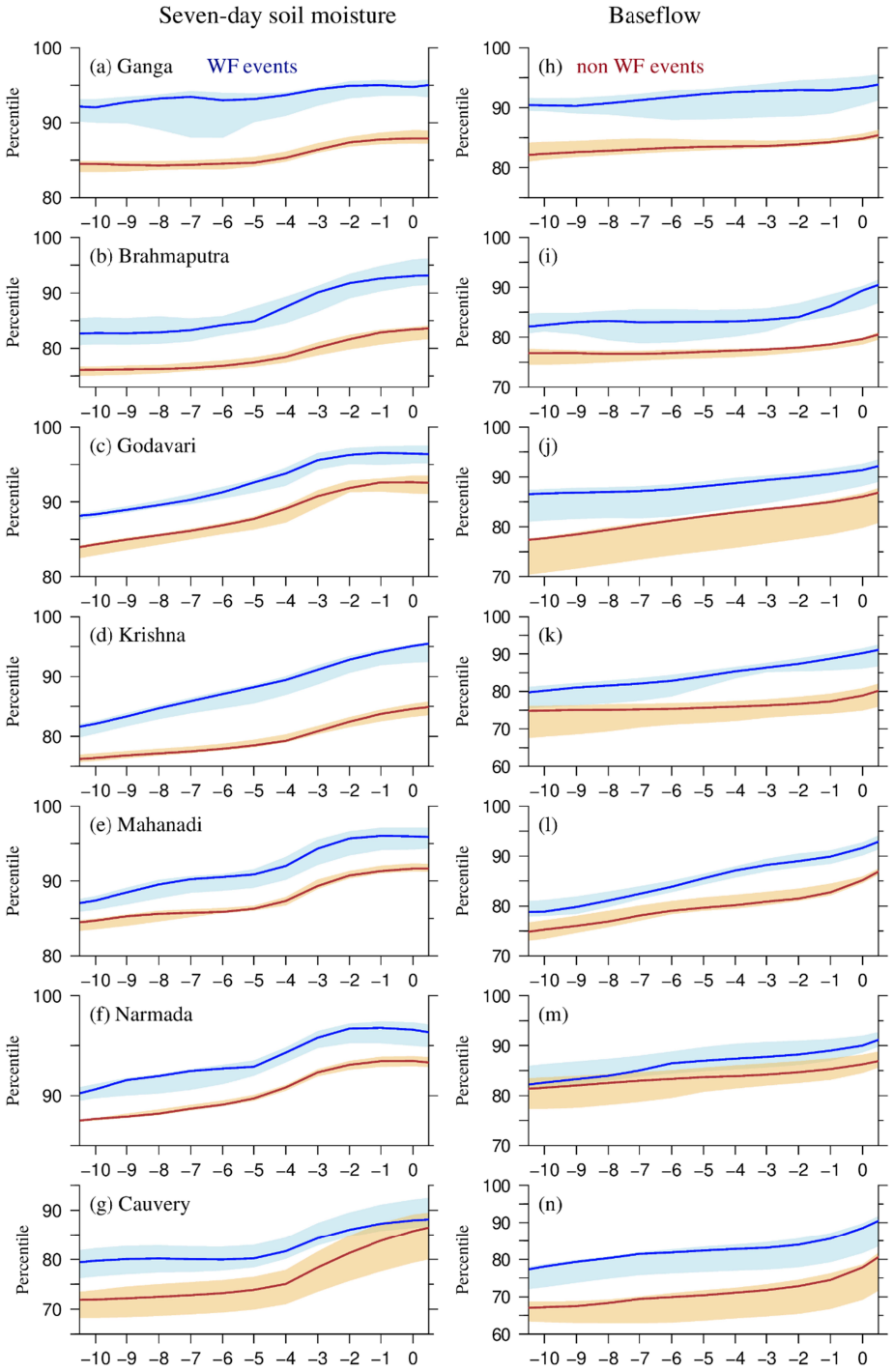

385

386 **Figure 4. Antecedent soil moisture and baseflow conditions.** Figures (a-g) show the
387 composite of seven-day mean soil moisture percentiles 10 days before the precipitation to day
388 0 before widespread floods (blue color) and high flows that do not cause widespread floods
389 (brown color) for each basin. The thick line shows the median soil moisture percentile on
390 each day for all the sub-basins within a basin. The shading shows the 25th and 75th percentile
391 of soil moisture of all the sub-basins. The uncertainty band depicts the variability across the

sub-basins. Figures (h-n) show the same for the antecedent baseflow conditions. Eckhardt's digital filter is used for estimating the base flow from routed VIC streamflow simulations.

3.4. Atmospheric and oceanic drivers of widespread flooding.

We assessed the hydrometeorological drivers determining the seasonality and variability of widespread flood probability. Further, we evaluate the atmospheric and oceanic conditions, for which we selected the top widespread flooding events in all the seven subbasins in terms of the areal coverage and magnitude. We investigated the atmospheric characteristics — integrated water vapour transport (IVT) and mean sea level pressure anomaly — associated with the day of maximum catchment-averaged precipitation that drives widespread flooding. We find a unique atmospheric pattern related to widespread flooding in all the river basins, exhibiting a low-pressure system and high moisture transport (Figure 5 a-f). Further, in all seven basins except Cauvery, the movement of the southwest monsoon system that crosses the Indian peninsular region is evident (Figure 5f). We also observe a near-uniform distribution of precipitation over the river basins (Figure 5 h-n) associated with large-scale atmospheric circulations. Intense moisture transport is often associated with large-scale precipitation (Merz et al., 2021; Su et al., 2023; van der Wiel et al., 2018). The seven-day soil moisture percentiles depict a slow increase towards the day of maximum precipitation, highlighting the role of antecedent rainfall [Bloschl, 2022; Merz et al., 2021] (Figure 4 o-u). Overall, we observed intense moisture transport and wet antecedent conditions associated with the top widespread floods in all seven river basins.

Further, we assessed whether widespread flooding relates to larger oceanic circulations. We checked the association of the years in which widespread flooding occurred in each basin with ElNino, LaNina, Neutral, positive Indian Ocean Dipole (IOD), and negative IOD years. We considered only widespread floods wherein any subbasin within a basin registered high flows exceeding a return period of 20 years to ensure event rarity. We did not find any specific association between the occurrence of widespread flooding the prominent oceanic circulations. The lack of association implies that the occurrence of widespread flooding is more associated with the existence of favorable antecedent catchment moisture conditions and precipitation.

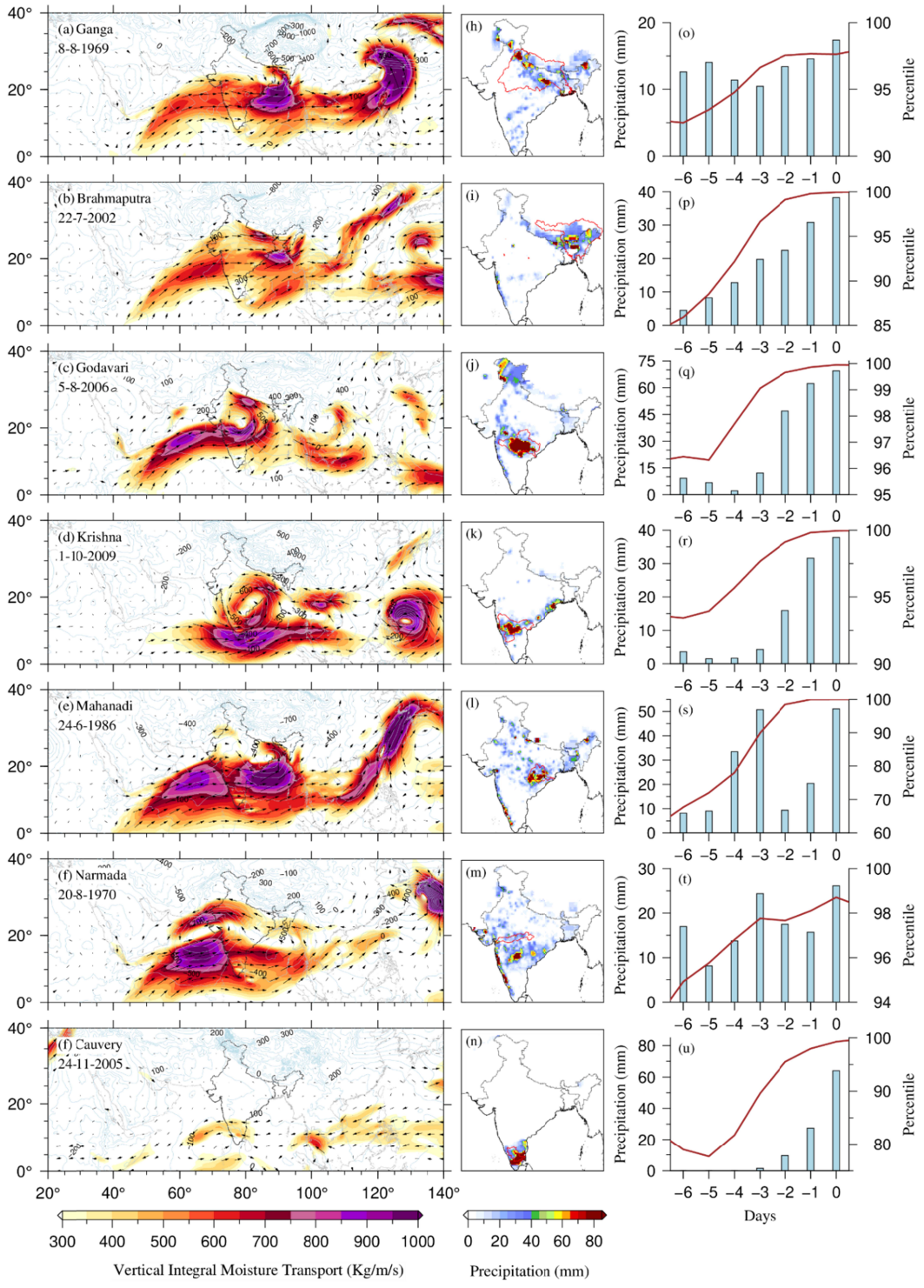

Figure 5. Atmospheric and catchment characteristics associated with WF events. We considered a single WF event in each basin with the highest fractional area and RP and identified the associated precipitation event. Figures (a-g) show the mean sea level pressure anomaly (blue contours) and integrated vertical moisture transport (IVT) [both vectors and shading] on the day of maximum catchment averaged precipitation (day 0). Figures (h-n)

show the spatial distribution of precipitation on the same day. Figures (o-u) show the precipitation hyetograph six days before the precipitation to day 0 (blue bars) and the seven-day mean soil moisture percentile (brown line) for the same period.

Regional variability in the onset, intensity, rainfall distribution, and length of dry and wet spells are observed over the Indian region (Ghosh et al., 2011; B. N. Goswami et al., 2006; Krishnamurthy et al., 2009; Malik et al., 2016). A change in the precipitation pattern has been observed in northeast India in the recent decades (1973-2019), reportedly connected to the changes in the surface temperature of the Arabian sea (Kuttippurath et al., 2021). Vinnarasi & Dhanya (2016) reported an increase in the duration of dry spells, intensification of precipitation during wet spells and temporal shifts in precipitation patterns during the summer monsoon season. In addition to climate forcing, direct anthropogenic factors such as land use and land cover changes, urbanization, and local changes in aerosol concentrations influence the precipitation variability observed over India adding further complexities to monsoon prediction (Vinnarasi & Dhanya, 2016). The changes in the onset of the summer monsoon and spatial and temporal variability within the monsoon season would alter the timing and probability of widespread flooding (Hrudya et al., 2021; Malik et al., 2016; Mishra, 2018).

3.5. Mechanisms of widespread flooding

Finally, we test the following hypothesis to understand the driving mechanism of widespread flooding in different catchments. We hypothesize that widespread flooding can occur in two scenarios; (I) widespread floods driven by rare high flow events in fewer subbasins and (II) widespread floods caused due to the simultaneous occurrence of low return period flows among most subbasins. In the peninsular rivers, more than half of the total widespread flooding is caused by scenario II (Figure 6 c-g). Less than half (quarter) of the widespread flooding results from at least one subbasin recording return period greater than 10 (RP >20) [Figure 6]. However, in the Ganga basin, in all the widespread flooding (in 3 of the 7 events) at least one subbasin records a return period greater than 10 (RP >20), while in the Brahmaputra basin, 75% (38%) of widespread flooding are driven by high flows with RP greater than 10 (RP>20) (Figure 6 a-b). We can ascertain that the widespread floods probability in large river basins highly depends on rare events in a few subbasins. In contrast, the peninsular rivers are less dependent on extreme events.

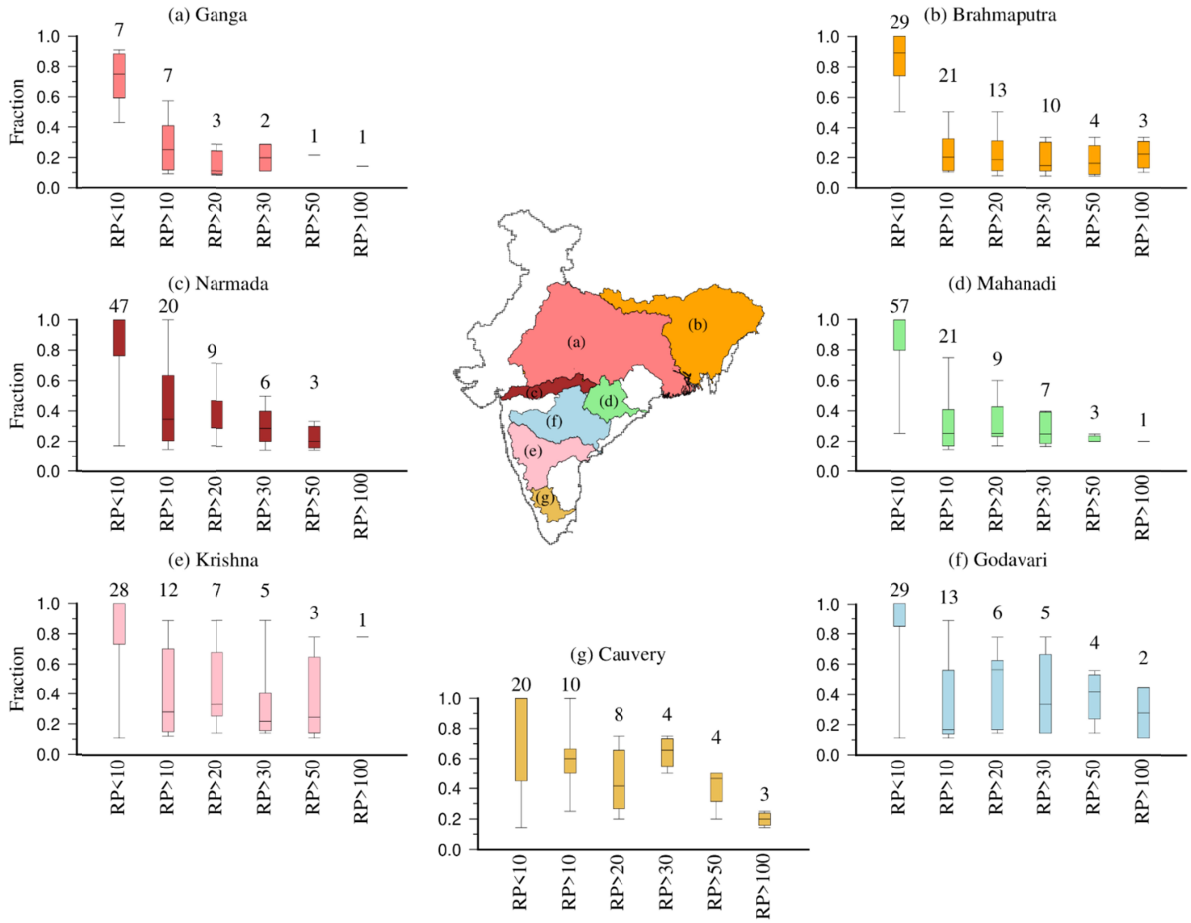

Figure 6. Return period of widespread floods. Figures (a-g) show the fraction of all sub-basins within a basin that experience widespread flooding with return period in a particular category. The number corresponding to the bar depicts the sample size. For instance, Figure 3(a) shows that of the 7 widespread floods in the Ganga basin, at least one subbasin experienced a RP below 10 (above 10). Similarly, in 3 widespread floods in the Gangetic basin, at least one subbasin experienced a RP above 20. Note that the fraction mentioned here is not the area-weighted fraction used to determine widespread floods. The boxes indicate the 25th and 75th percentiles, the horizontal line indicates the median and the whiskers correspond to the minimum and maximum fractions.

The Brahmaputra has the highest fraction of the area exposed to low-intensity precipitation (Figure S2). Therefore, despite having an increased number of rainy days in the Brahmaputra basin, due to the predominance of low-intensity precipitation —especially in the upper parts of the basin— the widespread flood probability becomes lower (see section 3.2). The Ganga basin, with fewer rainy days and a high percentage of low-intensity precipitation, similarly reduces the widespread flood probability. On the other hand, in the peninsular river basins,

low-intense precipitation and corresponding low flows most often drive widespread flooding and hence have a high widespread flood probability.

The projected changes in the intensity, magnitude and pattern of precipitation distribution in a warming climate could alter the seasonality and magnitude of widespread floods probability (Chinita et al., 2021; Hirabayashi et al., 2021; Pfahl et al., 2017; Trenberth et al., 2003). Rarely events in fewer subbasins drive widespread floods in large river basins like Brahmaputra and Ganga. In contrast, the simultaneous occurrence of the low return period (return period <10) flows most often drives widespread floods in the peninsular river basins. There is a high probability of an increase in the magnitude of rare extreme precipitation events in a warming climate (Barbero et al., 2017; Myhre et al., 2019; Papalexiou & Montanari, 2019; Zhang & Zhou, 2019). Goswami et al. (2006) reported an increase in the frequency and magnitude of extreme precipitation and a decrease in moderate precipitation over the Indian region. Extreme precipitation and consequent flows in the upper parts of a basin could, therefore, trigger more widespread flooding in a warming climate in the large river basins.

4. Conclusions

We identified the major drivers and mechanisms of widespread flooding in the Indian subcontinental river basins. There is a high probability of widespread flooding across all seven river basins during the summer monsoon season. We found that the spatial pattern of precipitation, antecedent moisture conditions, and the return period of streamflow in different subbasins influence the seasonality and variability of widespread floods in different river basins. Moreover, widespread flooding is associated with intense moisture transport and large atmospheric circulations. Understanding the drivers of widespread flooding in the observed climate is imperative to evaluate the projected changes in these drivers in a warming climate. The future changes in the drivers of widespread flooding would aid in determining the changes in widespread flooding and deciding adequate catchment scale management policies (Villarini & Wasko, 2021).

Other critical natural factors may control the widespread floods in a basin, such as the stream network pattern and density, the topography of a basin, and geomorphological characteristics (Brunner et al., 2020). The stream network pattern and density determine the connectivity within each subbasin. Similarly, the slope of a catchment would determine the time of concentration. The geomorphological factors and other catchment attributes like topography

508 and stream density are crucial in determining the connectivity and hence the driving
509 mechanisms of flooding (Sofia & Nikolopoulos, 2020; Wang et al., 2021). In this study, we
510 have not considered the role of the geomorphological factors in deciding the WF probability.
511 However, these factors are relatively static, considering the dynamic nature of climatic
512 factors. We focus on the climatic and associated hydrological characteristics that could
513 decide WF probability, which is crucial from a climate change perspective. Further, we have
514 yet to consider the role of direct human factors like the construction of reservoirs and
515 barrages, which is a major limitation of the study. However, in this study, we intended to
516 identify the drivers of widespread flooding in natural conditions during the observed climate.
517 Based on our findings the following conclusions can be made:

518 1. We found the peninsular river basins have a high widespread flooding probability
519 (>15%). In contrast, the widespread flooding probability in the Ganga and
520 Brahmaputra river basins is less than 10%. However, most river basins exhibit a high
521 probability of widespread flooding during the summer monsoon season, with
522 widespread flooding probability in peninsular rivers approaching 20%. The high
523 seasonality observed in WF probability is linked to the temporal pattern of
524 precipitation and streamflow, and an associated increase in catchment wetness
525 conditions during the summer monsoon season (June-September)
526
527 2. The spatial pattern of precipitation and rainy days and the relative rareness of high
528 flows in different subbasins can explain the variability of widespread flooding
529 probability across the river basins. Rare flows in a few subbasins (RP>20) drive
530 widespread flooding in the large river basins of the Ganga and Brahmaputra. In
531 contrast, the simultaneous occurrence of low flows (RP<10) across the subbasins
532 drives widespread flooding in the peninsular basins. For example, the central Indian
533 river basins of Godavari, Narmada and Mahandi, with low spatial variability in total
534 precipitation and rainy days, have the highest widespread flooding probability. On the
535 contrary, despite having the highest number of rainy days, the Brahmaputra river
536 basins exhibit a low WF probability due to the large percentage of low-intensity
537 precipitation in the upper parts of the basin.
538
539 3. Besides, the top widespread floods in all river basins are driven by a near-uniform
540 spatial distribution of extreme precipitation connected to large-scale atmospheric

moisture transport. The projected changes in the identified drivers of widespread floods will alter the timing, occurrence and probability of widespread floods in a warming climate.

Data Availability Statement

The authors obtained gridded precipitation and temperature data from IMD (https://dsp.imdpune.gov.in/). Streamflow observations from India Water Resources Information system (IWRIS; https://indiawris.gov.in/wris). The subbasins used in the study is downloaded from hydro basins (https://www.hydrosheds.org/products/hydrobasins)

Acknowledgement

The funding for the work from the Monsoon Mission Project, Ministry of Earth Sciences, is greatly appreciated.

Conflict of interest: The authors declare no competing interest.

Reference

Alfieri, L., Bisselink, B., Dottori, F., Naumann, G., de Roo, A., Salamon, P., et al. (2017). Global projections of river flood risk in a warmer world. *Earths Future*, *5*(2), 171–182. https://doi.org/10.1002/2016ef000485

Ali, H., & Mishra, V. (2018). Increase in Subdaily Precipitation Extremes in India Under 1.5 and 2.0 °C Warming Worlds. *Geophysical Research Letters*, *45*(14), 6972–6982. https://doi.org/10.1029/2018GL078689

Barbero, R., Fowler, H. J., Lenderink, G., & Blenkinsop, S. (2017). Is the intensification of precipitation extremes with global warming better detected at hourly than daily resolutions? *Geophysical Research Letters*, *44*(2), 974–983. https://doi.org/10.1002/2016GL071917

Berghuijs, W. R., Woods, R. A., Hutton, C. J., & Sivapalan, M. (2016). Dominant flood generating mechanisms across the United States. *Geophysical Research Letters*, *43*(9), 4382–4390. https://doi.org/10.1002/2016GL068070

Berghuijs, W. R., Harrigan, S., Molnar, P., Slater, L. J., & Kirchner, J. W. (2019). The Relative Importance of Different Flood-Generating Mechanisms Across Europe. *Water Resources Research*, *55*(6), 4582–4593. https://doi.org/10.1029/2019WR024841

570 Berthet, L., Andréassian, V., Perrin, C., & Javelle, P. (2009). How crucial is it to account for
571 antecedent moisture conditions in flood forecasting? Comparison of event-based on
572 continuous approaches on 178 catchments. *Hydrol Earth Syst Sci*, *13*(6), 819–831.
573 https://doi.org/10.5194/hess-13-819-2009

574 Bertola, M., Viglione, A., Vorogushyn, S., Lun, D., Merz, B., & Blöschl, G. (2020). Do small
575 and large floods have the same drivers of change? A regional attribution analysis in
576 Europe. *Hydrology and Earth System Sciences*. https://doi.org/10.5194/hess-2020-396

577 Bloschl, G. (2022). *Three hypotheses on changing river flood hazards*. *Hydrology and Earth*
578 *System Sciences*. Retrieved from https://hess.copernicus.org/preprints/hess-2022-232/

579 Blöschl, G, Ardoin-Bardin, S., Bonell, M., Dorninger, M., Goodrich, D., Gutknecht, D., et al.
580 (2007). At what scales do climate variability and land cover change impact on flooding
581 and low flows? *Hydrological Processes*. https://doi.org/10.1002/hyp.6669

582 Blöschl, Günter, Gaál, L., Hall, J., Kiss, A., Komma, J., Nester, T., et al. (2015). Increasing
583 river floods: fiction or reality? *Wiley Interdisciplinary Reviews: Water*, *2*(4), 329–344.
584 https://doi.org/10.1002/wat2.1079

585 Blöschl, Günter, Hall, J., Viglione, A., Perdigão, R. A. P., Parajka, J., Merz, B., et al. (2019).
586 Changing climate both increases and decreases European river floods. *Nature*,
587 *573*(7772), 108–111. https://doi.org/10.1038/s41586-019-1495-6

588 Brunner, M. I., Papalexiou, S., Clark, M. P., & Gilleland, E. (2020). How Probable Is
589 Widespread Flooding in the United States? *Water Resources Research*, *56*(10),
590 e2020WR028096. https://doi.org/10.1029/2020WR028096

591 Chinita, M. J., Richardson, M., Teixeira, J., & Miranda, P. M. A. (2021). Global mean
592 frequency increases of daily and sub-daily heavy precipitation in ERA5. *Environmental*
593 *Research Letters*, *16*(7), 074035. https://doi.org/10.1088/1748-9326/AC0CAA

594 Coles, S. (2001). *An Introduction to Statistical Modeling of Extreme Values*. London:
595 Springer London. https://doi.org/10.1007/978-1-4471-3675-0

596 Collischonn, W., & Fan, F. M. (2012). Defining parameters for Eckhardt's digital baseflow
597 filter. *Hydrological Processes*, *27*(18), 2614–2622. https://doi.org/10.1002/HYP.9391

598 Eckhardt, K. (2008). A comparison of baseflow indices, which were calculated with seven
599 different baseflow separation methods. *Journal of Hydrology*, *352*(1–2), 168–173.

https://doi.org/10.1016/J.JHYDROL.2008.01.005

Ettrick, T. M., Mawdlsey, J. A., & Metcalfe, A. V. (1987). The influence of antecedent catchment conditions on seasonal flood risk. *Water Resources Research*, *23*(3), 481–488. https://doi.org/10.1029/WR023I003P00481

Fazel-Rastgar, F. (2020). Extreme weather events related to climate change: widespread flooding in Iran, March–April 2019. *SN Applied Sciences*, *2*(12), 2166. https://doi.org/10.1007/s42452-020-03964-9

Fukushima, A., Kanamori, H., & Matsumoto, J. (2019). Regionality of long-term trends and interannual variation of seasonal precipitation over India. *Progress in Earth and Planetary Science*, *6*(1), 1–20. https://doi.org/10.1186/S40645-019-0255-4/FIGURES/12

Garg, S., & Mishra, V. (2019). Role of Extreme Precipitation and Initial Hydrologic Conditions on Floods in Godavari River Basin, India. *Water Resources Research*, *55*(11), 9191–9210. https://doi.org/10.1029/2019WR025863

Ghosh, S., Das, D., Kao, S. C., & Ganguly, A. R. (2011). Lack of uniform trends but increasing spatial variability in observed Indian rainfall extremes. *Nature Climate Change 2012 2:2*, *2*(2), 86–91. https://doi.org/10.1038/nclimate1327

Gilleland, E., & Katz, R. (2016). extRemes 2.0: An Extreme Value Analysis Package in R. *Journal of Statistical Software*, *72*(8), 1–39. https://doi.org/doi:10.18637/jss.v072.i08.

Goswami, B. (1998). Interannual variations of Indian summer monsoon in a GCM: external conditions versus internal feedbacks. *J Clim*, *11*, 501–522.

Goswami, B. N., Venugopal, V., Sangupta, D., Madhusoodanan, M. S., & Xavier, P. K. (2006). Increasing trend of extreme rain events over India in a warming environment. *Science*, *314*(5804), 1442–1445. https://doi.org/10.1126/science.1132027

Goswami, Bhupendra Nath, Venugopal, V., Sengupta, D., Madhusoodanan, M. S., & Xavier, P. K. (2006). Increasing trend of extreme rain events over India in a warming environment. *Science*, *314*(5804), 1442–1445.

Hersbach, H., & Dee, D. J. E. N. (2016). ERA5 reanalysis is in production. *ECMWF Newsletter*, *147*(7), 5–6.

629 Hettiarachchi, S., Wasko, C., & Sharma, A. (2019). Can antecedent moisture conditions
630 modulate the increase in flood risk due to climate change in urban catchments? *Journal*
631 *of Hydrology*, *571*, 11–20. https://doi.org/10.1016/j.jhydrol.2019.01.039

632 Hirabayashi, Y., Alifu, H., Yamazaki, D., Imada, Y., Shiogama, H., & Kimura, Y. (2021).
633 Anthropogenic climate change has changed frequency of past flood during 2010-2013.
634 *Progress in Earth and Planetary Science*, *8*(1), 1–9. https://doi.org/10.1186/S40645-
635 021-00431-W/FIGURES/3

636 Hong, C. C., Hsu, H. H., Lin, N. H., & Chiu, H. (2011). Roles of European blocking and
637 tropical-extratropical interaction in the 2010 Pakistan flooding. *Geophysical Research*
638 *Letters*, *38*(13). https://doi.org/10.1029/2011GL047583

639 Hrudya, P. H., Varikoden, H., & Vishnu, R. (2021). A review on the Indian summer monsoon
640 rainfall, variability and its association with ENSO and IOD. *Meteorology and*
641 *Atmospheric Physics*, *133*(1), 1–14. https://doi.org/10.1007/S00703-020-00734-
642 5/FIGURES/7

643 Ivancic, T. J., & Shaw, S. B. (2015). Examining why trends in very heavy precipitation
644 should not be mistaken for trends in very high river discharge. *Climatic Change*, *133*(4),
645 681–693. https://doi.org/10.1007/S10584-015-1476-1/FIGURES/4

646 Katz, R. W., Parlange, M. B., & Naveau, P. (2002). Statistics of extremes in hydrology.
647 *Advances in Water Resources*, *25*(8–12), 1287–1304. https://doi.org/10.1016/S0309-
648 1708(02)00056-8

649 Kim, J., Johnson, L., Cifelli, R., Thorstensen, A., & Chandrasekar, V. (2019). Assessment of
650 antecedent moisture condition on flood frequency: An experimental study in Napa River
651 Basin, CA. *Journal of Hydrology: Regional Studies*, *26*, 100629.
652 https://doi.org/10.1016/J.EJRH.2019.100629

653 Krishnamurthy, C. K. B., Lall, U., & Kwon, H. H. (2009). Changing frequency and intensity
654 of rainfall extremes over India from 1951 to 2003. *J. Clim.*, *22*(18), 4737–4746.
655 https://doi.org/10.1175/2009jcli2896.1

656 Kuttippurath, J., Murasingh, S., Stott, P. A., Balan Sarojini, B., Jha, M. K., Kumar, P., et al.
657 (2021). Observed rainfall changes in the past century (1901–2019) over the wettest place
658 on Earth. *Environmental Research Letters*, *16*(2), 024018. https://doi.org/10.1088/1748-

9326/ABCF78

Lamb, R., Keef, C., Tawn, J., Laeger, S., Meadowcroft, I., Surendran, S., et al. (2010). A new method to assess the risk of local and widespread flooding on rivers and coasts. *Journal of Flood Risk Management*, *3*(4), 323–336. https://doi.org/10.1111/J.1753-318X.2010.01081.X

Lehner, B., G. G. (2013). Global river hydrography and network routing: baseline data and new approaches to study the world's large river systems. *Hydrological Processes*, *27*(15), 2171–2186. https://doi.org/https://doi.org/10.1002/hyp.9740

Liang, X., Lettenmaier, D. P., Wood, E. F., & Burges, S. J. (1994). A simple hydrologically based model of land surface water and energy fluxes for general circulation models. *Journal of Geophysical Research*, *99*(D7), 14415. https://doi.org/10.1029/94JD00483

Lohmann, D., Nolte-Holube, R., & Raschke, E. (1996). A large-scale horizontal routing model to be coupled to land surface parametrization schemes. *Tellus A: Dynamic Meteorology and Oceanography*, *48(5)*, 708–721. Retrieved from https://doi.org/10.3402/tellusa.v48i5.12200

Lyngwa, R. V., & Nayak, M. A. (2021). Atmospheric river linked to extreme rainfall events over Kerala in August 2018. *Atmospheric Research*, *253*, 105488. https://doi.org/https://doi.org/10.1016/j.atmosres.2021.105488

Malik, N., Bookhagen, B., & Mucha, P. J. (2016). Spatiotemporal patterns and trends of Indian monsoonal rainfall extremes. *Geophysical Research Letters*, *43*(4), 1710–1717. https://doi.org/10.1002/2016GL067841

Martius, O., Sodemann, H., Joos, H., Pfahl, S., Winschall, A., Croci-Maspoli, M., et al. (2013). The role of upper-level dynamics and surface processes for the pakistan flood of July 2010. *Quarterly Journal of the Royal Meteorological Society*, *139*(676), 1780–1797. https://doi.org/10.1002/qj.2082

Merz, B., Blöschl, G., Vorogushyn, S., Dottori, F., Aerts, J. C. J. H., Bates, P., et al. (2021). Causes, impacts and patterns of disastrous river floods. *Nature Reviews Earth & Environment*, *0123456789*. https://doi.org/10.1038/s43017-021-00195-3

Mishra, A. K. (2018). Quantifying the impact of global warming on precipitation patterns in India. *Royal Meteorological Society*, *26*(1), 153–160. https://doi.org/10.1002/MET.1749

689 Mondal, A., & Mujumdar, P. P. (2015). Modeling non-stationarity in intensity, duration and
690 frequency of extreme rainfall over India. *Journal of Hydrology*, *521*, 217–231.
691 https://doi.org/10.1016/J.JHYDROL.2014.11.071

692 Mondal, A., & Mujumdar, P. P. (2016). Detection of Change in Flood Return Levels under
693 Global Warming. *Journal of Hydrologic Engineering*, *21*(8), 04016021.
694 https://doi.org/10.1061/(ASCE)HE.1943-5584.0001326

695 Myhre, G., Alterskjær, K., Stjern, C. W., Hodnebrog, Marelle, L., Samset, B. H., et al.
696 (2019). Frequency of extreme precipitation increases extensively with event rareness
697 under global warming. *Scientific Reports 2019 9:1*, *9*(1), 1–10.
698 https://doi.org/10.1038/s41598-019-52277-4

699 Nanditha, J. S., & Mishra, V. (2022). Multiday Precipitation Is a Prominent Driver of Floods
700 in Indian River Basins. *Water Resources Research*, *58*(7), e2022WR032723.
701 https://doi.org/10.1029/2022WR032723

702 Nanditha, J. S., Rajagopalan, B., & Mishra, · Vimal. (2022). Combined signatures of
703 atmospheric drivers, soil moisture, and moisture source on floods in Narmada River
704 basin, India. *Climate Dynamics*, *58*. https://doi.org/10.1007/s00382-022-06244-x

705 Nash, J. E., & Sutcliffe, J. V. (1970). River flow forecasting through conceptual models part
706 I—A discussion of principles. *Journal of Hydrology*, *10*(3), 282–290.

707 Nijssen, B., Lettenmaier, D. P., Liang, X., Wetzel, S. W., & Wood, E. F. (1997). Streamflow
708 simulation for continental-scale river basins and radiative forcings) applications of the
709 model to the Columbia and annual flow volumes to within a few percent . Difficulties in
710 reproducing the Sa6ramento Model [Burnash is dominated using an, *33*(4), 711–724.

711 Ouarda, T. B. M. J., & Charron, C. (2019). Changes in the distribution of hydro-climatic
712 extremes in a non-stationary framework. *Scientific Reports 2019 9:1*, *9*(1), 1–8.
713 https://doi.org/10.1038/s41598-019-44603-7

714 Pai, D. S., Sridhar, L., Rajeevan, M., Sreejith, O. P., Satbhai, N. S., & Mukhopadyay, B.
715 (2014). Development of a new high spatial resolution (0.25° × 0.25°) Long Period
716 (1901-2010) daily gridded rainfall data set over India and its comparison with existing
717 data sets over the region. *Mausam*, *65*(1), 1–18.

718 Papalexiou, S. M., & Montanari, A. (2019). Global and Regional Increase of Precipitation

719 Extremes Under Global Warming. *Water Resources Research*, *55*(6), 4901–4914.
720 https://doi.org/10.1029/2018WR024067

721 Pathiraja, S., Westra, S., & Sharma, A. (2012). Why continuous simulation? The role of
722 antecedent moisture in design flood estimation. *Water Resources Research*, *48*(6), 6534.
723 https://doi.org/10.1029/2011WR010997

724 Pfahl, S., O'Gorman, P. A., & Fischer, E. M. (2017). Understanding the regional pattern of
725 projected future changes in extreme precipitation. *Nature Climate Change 2017 7:6*,
726 *7*(6), 423–427. https://doi.org/10.1038/nclimate3287

727 Rentschler, J., Salhab, M., & Jafino, B. A. (2022). Flood exposure and poverty in 188
728 countries. *Nature Communications*, *13*(1), 1–11. https://doi.org/10.1038/s41467-022-
729 30727-4

730 Saji, N., Goswami, B., Vinayachandran, P., & Yamagata, T. (1999). A dipole mode in the
731 tropical Indian Ocean. *Nature*, *401*, 360–363.

732 Sharma, A., Wasko, C., & Lettenmaier, D. P. (2018, November 1). If Precipitation Extremes
733 Are Increasing, Why Aren't Floods? *Water Resources Research*. Blackwell Publishing
734 Ltd. https://doi.org/10.1029/2018WR023749

735 Shukla, R. P., & Huang, B. (2016). Interannual variability of the Indian summer monsoon
736 associated with the air–sea feedback in the northern Indian Ocean. *Climate Dynamics*,
737 *46*(5–6), 1977–1990. https://doi.org/10.1007/S00382-015-2687-X/FIGURES/8

738 Sofia, G., & Nikolopoulos, I. (2020). floods and rivers: a circular causality perspective.
739 *Scientific Reports*, *10*(5175). https://doi.org/10.1038/s41598-020-61533-x

740 Srivastava, A. K., Rajeevan, M., & Kshirsagar, S. R. (2009). Development of a high
741 resolution daily gridded temperature data set (1969-2005) for the Indian region.
742 *Atmospheric Science Letters*, *10*(4), 249–254. https://doi.org/10.1002/asl.232

743 Su, Y., Smith, J. A., & Villarini, G. (2023). The Hydrometeorology of Extreme Floods in the
744 Lower Mississippi River. *Journal of Hydrometeorology*, *24*(2), 203–219.
745 https://doi.org/10.1175/JHM-D-22-0024.1

746 Tarasova, L., Merz, R., Kiss, A., Basso, S., Blöschl, G., Merz, B., et al. (2019). Causative
747 classification of river flood events. *Wiley Interdisciplinary Reviews: Water*, *6*(4), e1353.
748 https://doi.org/10.1002/wat2.1353

749 Tramblay, Y., Villarini, G., El Khalki, E. M., Gründemann, G., & Hughes, D. (2021).
750 Evaluation of the Drivers Responsible for Flooding in Africa. *Water Resources*
751 *Research*, *57*(6). https://doi.org/10.1029/2021WR029595

752 Trenberth, K. E., Dai, A., Rasmussen, R. M., & Parsons, D. B. (2003). The Changing
753 Character of Precipitation. *Bulletin of the American Meteorological Society*, *84*(9),
754 1205–1218. https://doi.org/10.1175/BAMS-84-9-1205

755 Vijaykumar, P., Abhilash, S., Sreenath, A. V., Athira, U. N., Mohanakumar, K., Mapes, B.
756 E., et al. (2021). Kerala floods in consecutive years - Its association with mesoscale
757 cloudburst and structural changes in monsoon clouds over the west coast of India.
758 *Weather and Climate Extremes*, *33*, 100339.
759 https://doi.org/10.1016/J.WACE.2021.100339

760 Villarini, G., & Wasko, C. (2021). Humans, climate and streamflow. *Nature Climate Change*,
761 *11*(9), 725–726. https://doi.org/10.1038/s41558-021-01137-z

762 Vinnarasi, R., & Dhanya, C. T. (2016). Changing characteristics of extreme wet and dry
763 spells of Indian monsoon rainfall. *Journal of Geophysical Research*, *121*(5), 2146–2160.
764 https://doi.org/10.1002/2015JD024310

765 Walker, G. T. (1925). Correlation in seasonal variations of weather—a further study of world
766 weather. *Mon Weather Rev*, (53), 252–254.

767 Wang, W. C., Zhao, Y. W., Xu, D. M., Chau, K. W., & Liu, C. J. (2021). Improved flood
768 forecasting using geomorphic unit hydrograph based on spatially distributed velocity
769 field. *Journal of Hydroinformatics*, *23*(4), 724–739.
770 https://doi.org/10.2166/HYDRO.2021.135

771 Wasko, C., & Nathan, R. (2019). Influence of changes in rainfall and soil moisture on trends
772 in flooding. *Journal of Hydrology*, *575*, 432–441.
773 https://doi.org/10.1016/j.jhydrol.2019.05.054

774 Wasko, C., Nathan, R., & Peel, M. C. (2020). Changes in Antecedent Soil Moisture Modulate
775 Flood Seasonality in a Changing Climate. *Water Resources Research*, *56*(3), no.
776 https://doi.org/10.1029/2019WR026300

777 van der Wiel, K., Kapnick, S. B., Vecchi, G. A., Smith, J. A., Milly, P. C. D., & Jia, L.
778 (2018). 100-Year Lower Mississippi Floods in a Global Climate Model: Characteristics

779 and Future Changes. *Journal of Hydrometeorology*, *19*(10), 1547–1563.
780 https://doi.org/10.1175/JHM-D-18-0018.1

781 Xie, J., Liu, X., Wang, K., Yang, T., Liang, K., & Liu, C. (2020). Evaluation of typical
782 methods for baseflow separation in the contiguous United States. *Journal of Hydrology*,
783 *583*(August 2019), 124628. https://doi.org/10.1016/j.jhydrol.2020.124628

784 Zhang, W., & Zhou, T. (2019). Significant Increases in Extreme Precipitation and the
785 Associations with Global Warming over the Global Land Monsoon Regions. *Journal of*
786 *Climate*, *32*(24), 8465–8488. https://doi.org/10.1175/JCLI-D-18-0662.1

787

788